Effect of Junction Point Functionality on the Lamellar Spacing of Symmetric $(PS)_n(PI)_n$ Miktoarm Star Block Copolymers

Yuqing Zhu and Samuel P. Gido*

Department of Polymer Science & Engineering, University of Massachusetts, Amherst, Massachusetts 01003

Maria Moshakou, Hermis Iatrou, and Nikos Hadjichristidis*

Department of Chemistry, University of Athens, Panepistimiopolis Zografou 15771, Athens, Greece

Soojin Park and Taihyun Chang

Department of Chemistry, Pohang University of Science & Technology, Pohang, Kyungbuk, Korea 790-784

Received May 5, 2003

ABSTRACT: To probe the effect of junction point functionality in miktoarm star block copolymer architecture on chain conformation and morphology, a series of A_nB_n miktoarm star copolymers where A arms are PS blocks and B arms are PI blocks were investigated. The overall series including a diblock and the star block copolymers can be represented by A_nB_n, where $n = 1$, 2, 4, and 16. These materials were produced by synthesizing a single batch of living PS arms and a single batch of living PI arms and then linking them together with chlorosilane coupling agents of different functionality. Thus, all PS arms are identical and all PI arms are identical across the entire series of materials. All stars in the series have equal numbers of PS and PI arms, and the volume fractions of all the samples in the series (nearly 0.50 PS by volume) are identical within experimental error. All the materials were found, via small-angle X-ray scattering and transmission electron microscopy, to form lamellar morphologies. A significant increase in lamellar spacing with increasing junction point functionality (n) was found in this series of materials and can be attributed to molecular crowding near the junction point.

Introduction

Miktoarm star block copolymers with the A_nB_n architecture, illustrated in Figure 1, have n arms of polymer A and n arms of polymer B connected at one central junction point. AB diblocks can be viewed as a special case of A_nB_n star block copolymers where n is equal to 1. Olvera de la Cruz and Sanchez[1] predict that near 0.5 component volume fractions the order−disorder transition temperatures (ODT) of A_nB_n star copolymers are independent of n, and the length scales of the morphologies in the weak segregation limit are also independent of n. Additionally, the strong segregation limit theory of Milner[2] for the morphologies of A_nB_n type of block copolymers neglects the effects of the junction point on chain conformation and thus predicts that A_nB_n miktoarm stars of all n values behave identically to the corresponding AB diblock copolymer, which has the same A arm and the same B arm.

Contrary to these early predictions, recent experimental results have shown that the lamellar long periods of A_nB_n miktoarm star copolymers are larger than their corresponding diblock copolymers.[3−7] Comparison among the results from different groups of A_nB_n star block copolymers[4] indicates that lamellar spacing increases with increasing values of n. The lamellar spacing discrepancy between the A_nB_n stars and their corresponding AB diblocks results from chain crowding near the central core, where multiple arms converge on the same junction point. For any A_nB_n architecture, we define the corresponding diblock to consist of one A and one B arm. The polymer chain segments near the junction point have to adopt a stretched trajectory away from the junction points, as in the case of a star molecule,[8] to minimize this chain crowding. This leads to an increase in lamellar spacing of star block copolymers compared to a corresponding diblock copolymer.

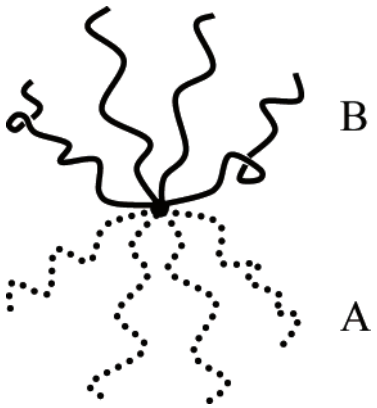

Figure 1. Illustration of an A_nB_n star block copolymer with $n = 4$.

It has been established that the discrepancy between AB diblock and A_2B_2 stars can be predicted by a self-consistent mean-field theory, and it is due to a reduction in the translational entropy of the junction point.[9] By adding this entropy term into the free energy equation, a strong segregation theory has been derived to explain the increase in domain spacing of A_2B_2 as compared to AB diblock copolymers. It has also been pointed out that the lamellar spacing difference between A_2B_2 and the corresponding AB diblock decreases with the increasing

* To whom correspondence should be addressed: spgido@squeaky.pse.umass.edu; hadjichristidis@chem.uoa.gr.

10.1021/ma030254f CCC: $25.00
Published on Web 07/03/2003

χN_0, where the N_0 is the degree of polymerization of the corresponding diblock copolymer and the χ is the Flory–Huggins interaction parameter. This supports the earlier observation[2,4] that this influence from the central core vanishes when the molecular weight of the corresponding diblock copolymer (or N_0) becomes very large. For molecules with high value of N_0, the lamellar spacing is larger because of the high molecular weight, but the increase in the spacing over that of the corresponding AB diblock decreases with increasing molecular weight. This trend has been proven by comparing the microdomain properties of three pairs of A_2B_2 stars and their corresponding AB diblocks.[3] The lamellar spacing ratio of the A_2B_2 stars to their corresponding AB diblocks decreases from 1.10 to 1.05 as the value of χN_0 increases from 12 to 73. A theoretical model was recently proposed to describe this extra stretching effect of star block copolymers with small to intermediate arm length based on the assumption of segmental mixing in an oblate ellipsoid volume located at the interface and centered on the junction point. It is predicted that the lamellar period for miktoarm stars increases as $f^{1/6}N^{2/3}\chi^{1/12}$, where f ($= 2n$) is the total number of both A and B arms.[7] On the basis of the previous research, it is clearly suggested that the lamellar spacing of A_nB_n stars is controlled by two independent parameters: the molecular weight of the corresponding AB diblock, which determines the segregation strength of the polymer segments, and the functionality (number of arms connected) at the central core.

However, for most of the systems studied, the corresponding AB diblock copolymers were either not available for direct comparison or synthesized in a different batch. The spacing differences between miktoarm star copolymers and diblocks were usually obtained by comparing experimental data from A_nB_n stars with the spacings of the calculated corresponding diblock copolymers based on their molecular weights and previously determined scaling relationships.[10] The objective of current work is to experimentally isolate the influence of functionality (n) on the lamellar morphologies of A_nB_n copolymers while holding the variables, such as arm molecular weight and composition, constant. To achieve this end, a series of $(PS)_n(PI)_n$ miktoarm star copolymers (n = 1, 2, 4, and 16) were synthesized utilizing anionic polymerization and chlorosilane coupling chemistry. The n equal to 1 case is the corresponding diblock copolymer for all the stars with higher n in this series. All the PS arms used in all the samples were obtained from the same anionically synthesized batch and thus were characteristically the same. Likewise, all the PI arms were also from the same batch. These arms were then linked together in different symmetric numbers using different cholorsilane coupling agents. To within experimental error, all samples have the same component volume fractions and differ only in the junction point functionality, allowing us to isolate the effect of the junction point on lamellar morphology.

Experimental Section

All reagents used were purified using standard techniques.[11,12] Manipulations were performed under high vacuum in glass vessels, washed with *n*-BuLi, and rinsed with benzene. Additions of reagents were made through break-seals and removals of materials were performed through heat-sealing of constrictions.[11,13,14] *s*-BuLi was prepared under vacuum from *sec*-butyl chloride and lithium dispersion and was used for initiating polymerization of PS and PI arms. The coupling agents—liquid chlorosilanes with 2 and 4 Si–Cl groups (for n = 1, 2)—were purified by fractional distillation on the vacuum line, diluted with benzene, and then subdivided into break-seal-equipped ampules. The synthesis of chlorosilane coupling agents with 8 and 32 Si–Cl groups (n = 4, 16) was accomplished according to methods reported previously.[15]

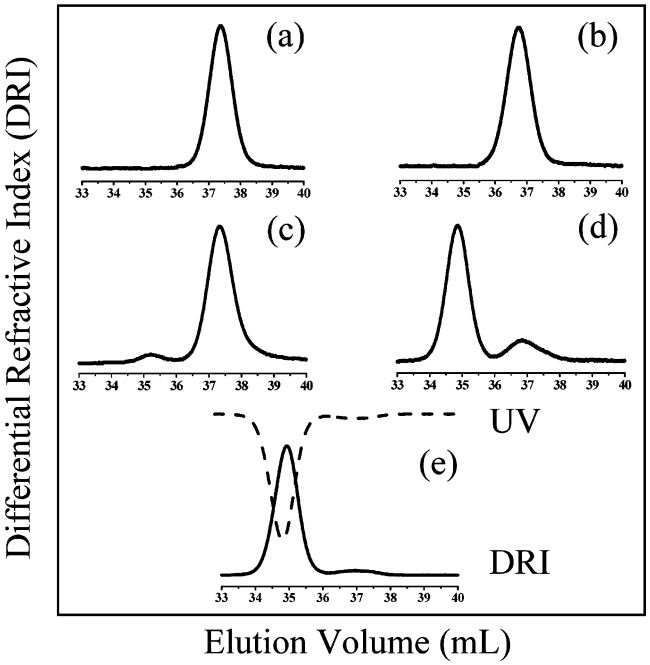

Figure 2. SEC chromatograms obtained during the synthesis ofthe PS–PI copolymer: (a) PS precursor, (b) PI precursor, (c) $(PS)Si(CH_3)_2Cl_2$, (d) unfractionated copolymer, and (e) fractionated copolymer.

The general reactions used for the synthesis of PS–PI diblock copolymer are given in Scheme 1.

Scheme 1

$$\text{styrene} + s\text{-BuLi} \rightarrow \text{PSLi}$$

$$\text{isoprene} + s\text{-BuLi} \rightarrow \text{PILi}$$

$$\text{PSLi} + \text{excess } SiCl_2(CH_3)_2 \rightarrow (PS)SiCl(CH_3)_2 + LiCl + SiCl_2(CH_3)_2\uparrow$$

$$(PS)SiCl(CH_3)_2 + \text{excess PILi} \rightarrow (PS)(PI)Si(CH_3)_2 + LiCl + \text{PILi}\downarrow$$

A benzene solution of the living PSLi was added to a large amount of dichlorodimethylsilane (ratio of Si–Cl groups to PSLi was about 100). This resulted in chlorosilane end-capped with a minimum of PS–PS block coupling. Excess linking agent was removed by extensive pumping on the vacuum line and by repeatedly dissolving the polymer and removing the solvent. Finally, a slight excess amount of living PILi chains was added to the macromolecular linking agent $(PS)Si(CH_3)_2$-Cl. The step-by-step synthetic procedure was monitored by size exclusion chromatography (SEC). Figure 2 shows the SEC analysis of the PS–PI diblock copolymer. While this is an unusually complicated procedure for the synthesis of a diblock copolymer, it was necessary in order to preserve structural consistency with the other materials in our A_nB_n series.

The reactions for the synthesis of $(PS)_2(PI)_2$ stars are given in Scheme 2.

Scheme 2

$$\text{PSLi} + SiCl_4 \rightarrow PSSiCl_3 + LiCl$$

$$\text{PSLi} + PSSiCl_3 \rightarrow (PS)_2SiCl_2 + LiCl$$

$$(PS)_2SiCl_2 + \text{excess PILi} \rightarrow (PS)_2Si(PI)_2 + 2LiCl + \text{PILi}\downarrow$$

Table 1. Molecular Characteristics of Miktoarm Star Copolymers and Precursors

					$(PS)_n(PI)_n$ star block copolymers					
		$(PS)_nCl_n$ intermediate						wt % PS		
sample	M_n[a] (g/mol)	M_n[a](g/mol)	M_w/M_n[e]	no. of PS arms/junction	M_n[a] (g/mol)	M_w[b] (g/mol)	M_w/M_n[e]	^{1}H NMR	UV[c]	calcd[d]
PS arms	19 000									
PI arms	15 000									
PS−PI		19 000	1.04	1.0	36 200	36 300	1.05	55 ± 2	54 ± 2	52
$(PS)_2(PI)_2$		38 000	1.04	2.0	64 000	66 000	1.04	56 ± 2	55 ± 2	58
$(PS)_4(PI)_4$		67 300	1.04	3.5	121 000	127 500	1.04	54 ± 2	52 ± 2	55
$(PS)_{16}(PI)_{16}$		301 200	1.03	15.8	*f*	533 000	1.07	59 ± 2	58 ± 2	56

[a] Number-averaged molecular weight measured using membrane osmometry (MO) in toluene at 35 °C. [b] Weight-averaged molecular weight measured using low-angle laser light scattering (LALLS) in THF at 25 °C. [c] Results measured using size exclusion chromatography in THF at 25 °C (UV detector). [d] Calculated PS weight faction wt % PS = $M_n(PS)_n \times 100/M_n$ star. [e] Determined via size exclusion chromatography in THF at 25 °C (DRI detector). [f] The molecular weight of the molecule is too high to be measured by MO.

A PSLi benzene solution was added into a solution of $SiCl_4$ in a ratio of $(SiCl_4)/(PSLi) = 3:1$. The resulting mixture of $(PS)_2SiCl_2$ and $PSSiCl_3$ was titrated with PSLi until nearly all the $PSSiCl_3$ was transformed into $(PS)_2SiCl_2$. The reaction is deterred from proceeding to the formation of $(PS)_3SiCl$ or $(PS)_4Si$ through the steric hindrance of the polystyryllithium anions. Finally, an excess of living PILi chains was added to the macromolecular linking agent $(PS)_2SiCl_2$ in order to react with the two remaining chloride functionalities, which leads to the formation of $(PS)_2Si(PI)_2$.

The syntheses of the remaining materials in the A_nB_n series were accomplished according to the reactions shown in Scheme 3 and the method described elsewhere.[16]

Scheme 3

$$n\text{PSLi} + \text{SiCl}_{2n} \rightarrow (\text{PS})_n\text{SiCl}_n + n\text{LiCl}$$

$$(\text{PS})_n\text{SiCl}_n + \text{excess PILi} \rightarrow (\text{PS})_n\text{Si(PI)}_n + n\text{LiCl}$$

The chlorosilane coupling agent $Si[CH_2CH_2Si(CH_3)Cl_2]_4$ was used for the synthesis of the $(PS)_4(PI)_4$ and $Si[CH_2CH_2Si(CH_3)\{CH_2CH_2Si(CH_3)[CH_2CH_2Si(CH_3)Cl_2]_2\}_2]_4$ for $(PS)_{16}(PI)_{16}$, respectively. These multifunctional chlorosilanes were prepared by using tetravinylsilane as the initial core molecule, methyldichlorosilane as the propagating units, and vinylmagnesium bromide for the transformation of the silicon chloride to the silicon vinyl group as described elsewhere.[15]

An appropriate quantity of living PSLi was added to the benzene solutions of the different chlorosilane coupling agents [(Si−Cl)/(PSLi) = 2:1.1] to ensure the formation of the $(PS)_n$-$SiCl_n$ stars. The progress of the formation of $(PS)_nSiCl_n$ was monitored using SEC and membrane osmometry (MO). As before, there is a sterically directed tendency for the reaction to stop after addition of one PS chain to each difunctional chlorosilane group of the linking agent. As an example, the SEC curves of the $(PS)_4(PI)_4$ miktoarm star copolymer, its precursor arms, and its intermediate product $(PS)_4SiCl_4$ are given in Figure 3. These reactions usually were completed in 1−2 days, and then an excess amount of PILi benzene solution was added to the reactor. Depending upon the number of arms, coupling reactions were completed in 1.5−2 months. Excess living PSLi and PILi arms were terminated by addition of degassed methanol. All the $(PS)_n(PI)_n$ star block copolymers were purified by fractionation.

SEC experiments were carried out at 25 °C in THF, using a Waters 410 SEC with a differential refractometer detector, a UV detector, and six columns with porosity ranges from 10^2 to 10^6 Å. Number-average molecular weights (M_n) of the precursor arms, the intermediates, and the final products were also measured with a Jupiter model 231 recording membrane osmometer (MO) at 35 °C. Weight-average molecular weights (M_w) of the $(PS)_n(PI)_n$ star copolymers were measured at 25 °C using a Chromatix KMX-6 low-angle laser light scattering (LALLS) photometer at a wavelength of 633 nm. Molecular information on all the materials is listed in Table 1. PS weight fractions were determined by ^{1}H NMR analysis using a Bruker AC 200 instrument in $CDCl_3$ at 30 °C. PS volume fractions were calculated on the basis of ^{1}H NMR and GPC−UV results.

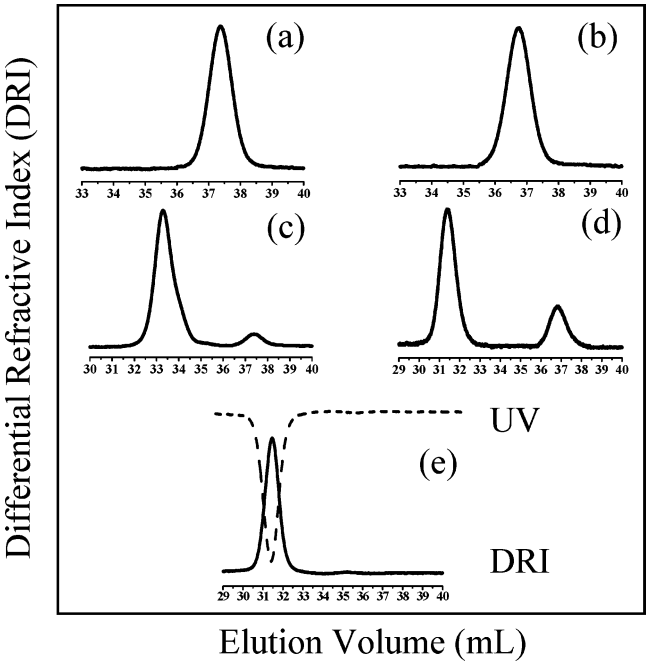

Figure 3. SEC chromatograms during the synthesis ofthe $(PS)_4(PI)_4$ miktoarm star copolymer: (a) PS arm, (b) PI arm, (c) $Si[CH_2CH_2Si(CH_3)(PS)Cl]_4$ intermediate macromolecule, (d) unfractionated $(PS)_4(PI)_4$ star block copolymer, and (e) fractionated $(PS)_4(PI)_4$ copolymer.

The experimental error for ^{1}H NMR or GPC−UV analysis is about ±2%, which leads to ±2% error in the calculated PS volume fractions.

The successful establishment of the scale law of lamellar spacing on the functionality of the star block copolymers relies on the successful synthesis of the $(PS)_n(PI)_n$ star copolymers, without serious contamination by star block copolymers with other component combinations, such as $(PS)_{n+1}Si(PI)_{n-1}$ or $(PS)_{n-1}Si(PI)_{n+1}$ or other combinations. To probe this composition fluctuation in the materials we studied, temperature gradient liquid chromatography (TGLC) was carried out on a typical HPLC system equipped with a C18 bonded silica column (Alltech, Platinum EPS C18, 100 Å pore, 53 × 7.0 mm i.d., 3 μm particle size). The mobile phase was 1,4-dioxane, and the temperature of the column was linearly raised from 15 to 45 °C throughout the experiment as shown in Figure 4 for star block copolymers with $n = 2$, 4, and 16. Gaussian peak deconvolution was used to calculate the percentage of each structure in the HPLC chromatogram. The purity of $(PS)_2(PI)_2$ is determined to be 74% with some contamination of PS and PI homopolymers, while that of $(PS)_4(PI)_4$ is 57% with 16% of $(PS)_4(PI)_3$ and 20% of $(PS)_3(PI)_4$ as major side products. The molecular weight of $(PS)_{16}(PI)_{16}$ is too high to be analyzed using the TGLC method. On the basis of these analyses, we conclude that there is inherent contamination resulting from the synthesis of miktoarm stars of this type. These contamination

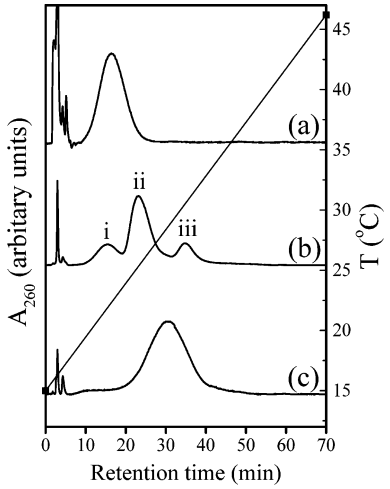

Figure 4. Temperature gradient liquid chromatography (TGLC) analyses of the star block copolymers (n = 2, 4, 16): (a) $(PS)_2(PI)_2$, with $(PS)_2(PI)_2$ at 74%; (b) $(PS)_4(PI)_4$, (i) 16% of $(PS)_3(PI)_4$, (ii) 57% of $(PS)_4(PI)_4$, and (iii) 20% of $(PS)_4(PI)_3$; (c) $(PS)_{16}(PI)_{16}$.

species are resistant to detection via standard SEC and to separation by standard methods such as solvent−nonsolvent fractionation. All previous results reported in the literature regarding miktoarm stars obtained by methods were produced by similar synthetic routes, and thus these materials most likely had similar contamination.

Solutions of about 5 wt % copolymers in toluene were prepared. Bulk films about 1 mm thick were obtained by slowly evaporating the solvent from these solutions over a period of 14 days at room temperature. The dried films thus obtained were annealed at 120 °C under vacuum for 7 days to promote equilibrium structures. All samples for transmission electron microscopy (TEM) study were microtomed using a Leica Ultracut UCT cryoultramicrotome. Thin sections 50−100 nm in thickness were cut with a Diatome diamond knife at a sample temperature of −110 °C and a knife temperature of −100 °C. These sections were collected on TEM grids and stained in OsO_4 vapor for 6 h. TEM was performed on a JEOL 100 CX, operated at an accelerating voltage of 100 kV.

Small-angle X-ray scattering (SAXS) data were collected using Ni-filtered Cu Kα radiation (λ = 1.54 Å) from a Rigaku rotating anode operated at 40 kV and 200 mA. The primary beam was collimated by a set of three pinholes. A gas-filled area detector (Siemens Hi-Star), located 87.52 cm from the sample, was used to record scattering patterns. The flight path between the sample and the detector was evacuated.

Results and Discussion

All the $(PS)_n(PI)_n$ miktoarm star copolymers (n = 1, 2, 4, and 16) form lamellar morphologies. Figure 5 shows a TEM micrograph of the lamellar structure observed in the $PS_{16}PI_{16}$ star copolymer. The SAXS plot in Figure 6 shows several higher order reflections in all materials, indicating that these materials are well-ordered. The different sets of SAXS data have been offset vertically for clarity. The second-order reflections of the three star block copolymers with low number of arms (n = 1, 2, 4) are suppressed, which indicates that the volume fractions of both blocks in these materials are nearly identical in the microphase-separated state. The copolymer with 32 arms is slightly more asymmetric in component volumes as the second reflection is readily seen in the profile. Determination of peak positions and thus lamellar spacing was conducted on Lorentz-corrected Iq^2 vs q plots. The scattering vectors divided by the orders of the respective peaks (q/n) were averaged over the primary and higher order peaks. This produced

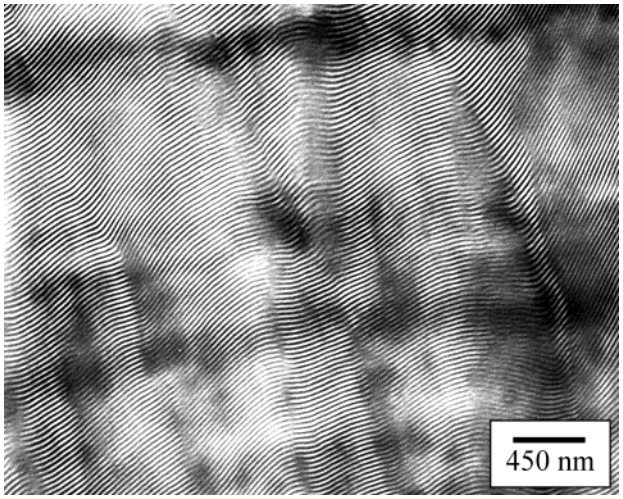

Figure 5. TEM image of $(PS)_{16}(PI)_{16}$ star block copolymer.

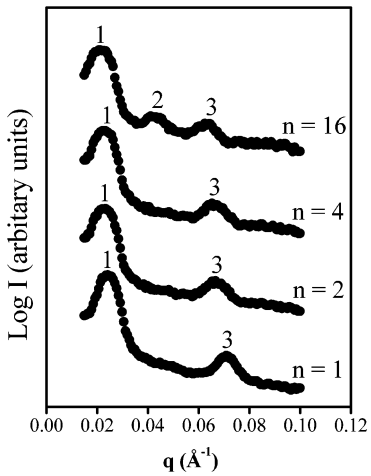

Figure 6. Small-angle X-ray scattering profiles of the $(PS)_n$-$(PI)_n$ star block copolymers.

an average value for the scattering vector of the primary peak, q^*, from which an average lamellar long period was calculated. The average q^* values and the corresponding lamellar long periods (D_n) are listed in Table 2. These results show that the lamellar spacing increases with increasing star functionality from 256 Å for the PS−PI diblock to 287 Å for the $(PS)_{16}(PI)_{16}$ star block copolymer. Standard deviations (σ) of the mean for the values of the q/n for the series of reflections can also be found in this table.

When comparing the spacings of lamellar morphologies across the A_nB_n series, we must consider the fact that the chlorosilane linking agent for higher n members has a significantly larger molecular diameter than for lower n members of the series. We must address the question of whether the increasing size of this linking agent contributes significantly to the increase in lamellar spacing with increasing n. To properly take the core size into account, the observed domain spacings are normalized by the unperturbed radius of gyration of a diblock consisting of one PS block, one PI block, and the average number of bonds linking these two arms through the core, $R_{g,n}$. For n = 1, and 2, this number of extra bonds to traverse the core is constant for any combination of one PS and one PI arm. However, for n = 4 and 16, there are different possible paths across the core that lead to different numbers of extra bonds. Table 2 lists the extra number of bonds in the core

Table 2. Morphological Characteristics of Miktoarm Star Copolymers

	PS (vol %)[a]	av q^* (Å^{-1})	σ of (q/n)[b]	D_n (Å)[c]	no. of Si−C at core[d]	no. of C−C at core[d]	N_n[e] (core)	$R_{g,n}$[f] (Å)	$(D_n/R_{g,n})/(D_1/R_{g,1})$
PS−PI	51 ± 2	0.0246	0.0013	256	2	0	0.67	56.2	1
$(PS)_2(PI)_2$	52 ± 2	0.0234	0.0010	269	2	0	0.67	56.2	1.05
$(PS)_4(PI)_4$	50 ± 2	0.0231	0.0004	271	5	0	2.33	56.3	1.06
$(PS)_{16}(PI)_{16}$	55 ± 2	0.0219	0.0008	287	10.6	4.3	4.97	56.5	1.12

[a] PS volume fraction, calculated based on the average results of ^{1}H NMR and SEC−UV analyses. [b] Standard deviation of the mean for q/n values. [c] Lamellar long period, calculated based on average q^*. [d] Extra bonds provided by the core structure. The number is averaged among all the probabilities of the arm combinations. [e] Degree of polymerization of the core structure. It is calculated from N = [(no. of Si−C bond) + (no. of C−C bond)]/3. [f] Radius of gyration of star block copolymers. $R_{g,n}^2 = [a_{av}(N_a + N_b + N_n)^2]/6$, where the a_{av} is the averaged Kuhn length of PS and PI in this series $a_{av} = (a_aN_a + a_bN_b)/(N_a + N_b)$. The a_a and a_b, N_a and N_b are the Kuhn length and the degree of polymerization of PS and PI arm, respectively.

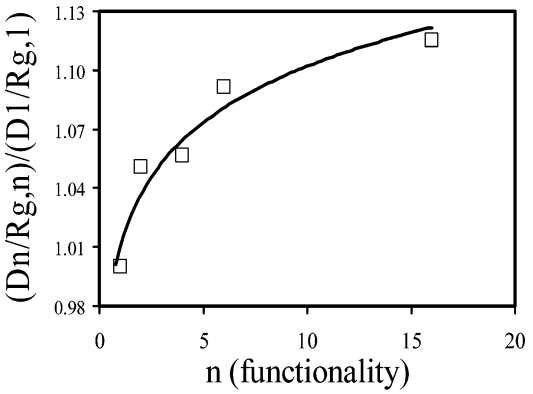

Figure 7. Plot of the normalized lamellar long periods ($D_n/R_{g,n}$) of $(PS)_n(PI)_n$ star copolymers (n = 1, 2, 4, 16) divided by that of the diblock member of the series ($D_1/R_{g,1}$) against the respective star functionality (n).

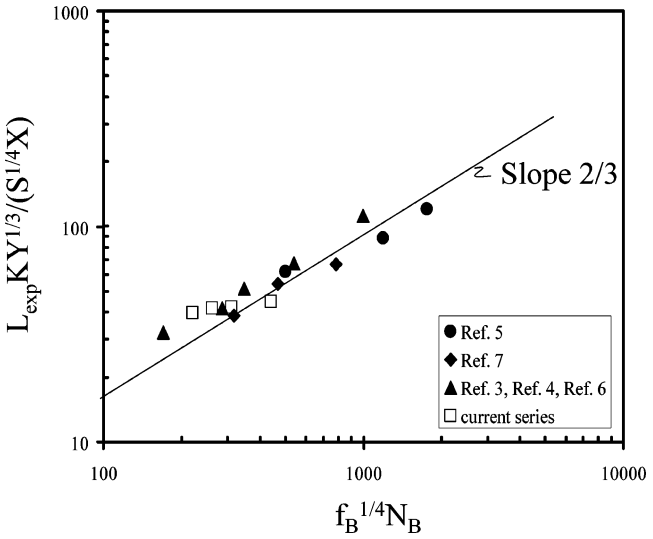

Figure 8. Experimental data mapped onto the log−log plot of modified lamellar period $[L_{exp}KY^{1/3}/(S^{1/4}X)]$ vs $f_B^{1/4}N_B$.

including averages over all combinations of PS and PI block locations for the n = 4 and 16 case. The table also lists the values of $R_{g,n}$; these values clearly do not increase significantly even when comparing the n = 1 case to the n = 16 case.

Figure 7 is a plot of the lamellar long periods of $(PS)_n$-$(PI)_n$ star copolymers normalized with respect to the corresponding diblock radius of gyration including the core size ($D_n/R_{g,n}$) vs n. This value is further normalized by ($D_1/R_{g,1}$), the value of this ratio for the corresponding diblock of the series. After the correction from the increased size of the coupling agent, it is clearly shown in Figure 7 that the lamellar spacing increases with the functionality of the center core and the curve plateaus at higher n. The experimental data were also mapped onto the log−log plot of lamellar period vs $f_B^{1/4}N_B$ as described by Grayer et al.,[7] which is shown in Figure 8. We conclude that the data from current series falls in a similar range as previous data. However, the limited range of $f_B^{1/4}N_B$ covered by our data makes it impossible to evaluate our data agreement with the Grayer theory.

Conclusions

Lamellar morphologies of a series of $(PS)_n(PI)_n$ star block copolymers (n = 1, 2, 4, and 16) with identical PS arms and identical PI arms, prepared by anionic polymerization and controlled chlorosilane chemistry, have been investigated. The materials were in the intermediate segregation regime and had nearly 50/50 volume fractions. Lamellar long periods of structures formed by the star copolymers (n > 1) were found to exceed that of the corresponding diblock copolymer (n = 1) and to increase with increasing number of arms at the central core. The relationship between the lamellar long period of these star copolymers and star functionality has been studied via SAXS results. However, the presence of side products with unintended A or B arm numbers appears to be an unavoidable consequence of the synthetic coupling strategy. These side products are often not completely separable by solvent−nonsolvent fractionation. These caveats apply not just to the materials of the current study but also to materials from previous reported work on A_nB_n stars in which the materials were synthesized by similar approaches.[3−7] Although the data from this study and the previous studies generally follows the theoretical prediction for crowding near the star junction point,[3−7] it is questionable as to whether a true test of the theory can be achieved until a cleaner synthesis of A_nB_n materials is available.

Acknowledgment. S.P.G. acknowledges funding from the U.S. Army Research Office under Contract DAAD-19-01-1-0544. H.I. and N.H. acknowledge the Ministry of Education for financial support through the Operational Program and Initial Educational Vocational Training on "Polymer Science and its Applications" (Graduate Program). The authors acknowledge Prof. T. P. Russell for the helpful discussion on small-angle X-ray scattering. The authors also acknowledge the use of central facility and the W. M. Keck Electron Microscopy in the Material Research Science and Engineering Center (MRSEC) at the University of Massachusetts—Amherst.

References and Notes

(1) Olvera de la Cruz, M.; Sanchez, I. C. *Macromolecules* **1986**, *19*, 2501.

(2) Milner, S. *Macromolecules* **1994**, *27*, 2333.
(3) Buzza, D. M. A.; Fzea, A. H.; Allgaier, J. B.; Young, R. N.; Hawkins, R. J.; Hamley, I. W.; McLeish, T. C. B.; Lodge, T. P. *Macromolecules* **2000**, *33*, 8399.
(4) Beyer, F. L.; Gido, S. P.; Uhrig, D.; Mays, J. W.; Beck Tan, N.; Trevino, S. F. *J. Polym. Sci., Part B: Polym. Phys.* **1999**, *37*, 3392.
(5) Beyer, F. L.; Gido, S. P.; Poulos, Y.; Avgeropoulos, A.; Hadjichristidis, N. *Macromolecules* **1997**, *30*, 2373.
(6) Turner, C. M.; Sheller, N. B.; Foster, M. D.; Lee, B.; Corona-Galvan, S.; Quirk, R. P.; Annis, B.; Lin, J. S. *Macromolecules* **1998**, *31*, 4372.
(7) Grayer, V.; Dormidontova, E. E.; Hadziioannou, G. *Macromolecules* **2000**, *33*, 6330.
(8) Daoud, M.; Cotton, J. P. *J. Phys. (Paris)* **1982**, *43*, 531.
(9) Matsen, M. W.; Gardiner, J. M. *J. Chem. Phys.* **2000**, *113*, 1673.
(10) Hashimoto, T.; Shibayama, M.; Kawai, H. *Macromolecules* **1980**, *12*, 1237.
(11) Hadjichristidis, N.; Iatrou, H.; Pispas, S.; Pitsikalis, M. *J. Polym. Sci., Part A: Polym. Chem.* **2000**, *38*, 3211.
(12) Morton, M.; Fetters, L. J. *J. Rubber Chem. Technol.* **1975**, *48*, 359.
(13) Iatrou, H.; Hadjichristidis, N. *Macromolecules* **1992**, *25*, 4649.
(14) Roovers, J.; Toporowski, P. M. *Macromolecules* **1983**, *16*, 843.
(15) Zhou, L.; Roovers, J. *Macromolecules* **1993**, *26*, 963.
(16) Averopoulos, A.; Poulos, Y.; Hadjichristidis, N.; Roovers, J. *Macromolecules* **1996**, *29*, 6076.

MA030254F